Improved ultrasound attenuation measurement method for the non-invasive evaluation of hepatic steatosis using FibroScan ®

Stéphane Audière, Aymeric Labourdette, Véronique Miette, Céline Fournier, Redouane Ternifi, Salem Boussida, Philippe Pouletaut, Fabrice Charleux, Sabine Bensamoun, Stephen A Harrison, et al.

Improved ultrasound attenuation measurement method for the non-invasive evaluation of hepatic steatosis using FibroScan®

Stéphane Audière[a], Aymeric Labourdette[a], Véronique Miette[a], Céline Fournier[a], Redouane Ternifi[b,1], Salem Boussida[b,2], Philippe Pouletaut[b], Fabrice Charleux[c], Sabine F.Bensamoun[b], Stephen A.Harrison[d] and Laurent Sandrin[a]

[a] Echosens, Paris, France;

[b] Université de technologie de Compiègne, CNRS, Biomechanics and Bioengineering, Centre de recherche Royallieu, CS 60319, 60203 Compiègne Cedex, France;

[c] ACRIM-Polyclinique Saint Côme, Medical Radiology, Compiègne, France;

[d] Radcliffe Department of Medicine, University of Oxford, UK;

Corresponding author:
Stéphane Audière
Postal address: 6 rue Ferrus, 75014 Paris, France
Telephone number: +33 1 44 82 78 50
E-mail address: stephane.audiere@echosens.com

In preparation for Ultrasound in Medicine and Biology

---

[1] Present Address: Mayo Clinic Rochester, Rochester, Minnesota, USA
[2] Present Address: Centre hospitalier universitaire Amiens-Picardie, France

Abstract

Controlled Attenuation Parameter (CAP) is a measurement of ultrasound attenuation used to assess liver steatosis non-invasively. However, the standard method has some limitations. We aimed to assess the performance of a new CAP method by ex vivo and in vivo assessments. The major difference with the new method is that it uses ultrasound data continuously acquired during the imaging phase of the FibroScan examination. Seven reference tissue-mimicking phantoms were used to test the performances. In vivo performances were assessed on two cohorts (in total 195 patients) of patients using magnetic resonance imaging proton density fat fraction (MRI-PDF) as a reference. The precision of CAP was improved by more than 50% on tissue-mimicking phantoms and between 22% and 41% in the in vivo cohort studies. The agreement between both methods was excellent and the correlation between CAP and MRI-PDFF improved in both studies (0.71 to 0.74, 0.70 to 0.76). Using MRI-PDFF as a reference, the diagnostic performance of the new method was at least equal or superior (area under the receiver operating curve 0.889 to 0.900, 0.835 to 0.873). This study suggests that the new continuous CAP method can significantly improve the precision of CAP measurements ex vivo and in vivo.

Keywords

Ultrasound attenuation, Controlled Attenuation Parameter (CAP), Liver, Steatosis, Elastography, Vibration-Controlled Transient Elastography (VCTE), FibroScan, Proton Density Fat Fraction (PDFF).

Introduction

Nonalcoholic fatty liver disease (NAFLD) is a one of the leading causes of liver disease, found in 20-25% of adults in the developed world (Younossi, et al. 2016). About half of NAFLD patients are obese, with the prevalence of NAFLD in nonobese or lean patients at 15.7% and 10.2%, respectively (Harrison, et al. 2021). It has also been reported that 26% of American obese children have NAFLD (Elizabeth, et al. 2019). Thus, it has major health and economic burdens. The severity is worsened as NAFLD can go undetected for some time, increasing the risk of it developing into the more advance and progressive form of nonalcoholic steatohepatitis (NASH), which can manifested further into cirrhosis and liver cancer. A recent study (Harrison, et al. 2021) reported the overall prevalence of NAFLD was 38% and 14% for NASH confirmed by biopsy in a cohort of asymptomatic middle-aged American adults. NAFLD is defined as hepatic steatosis, which is the accumulation of triglycerides within hepatocytes that exceeds 5% of liver weight. Liver biopsy is the gold standard method to assess liver steatosis (Bravo, et al. 2001), but it carries strong limitations due to its invasiveness and potential sampling error (Ratziu, et al. 2005, Shahin Merat, et al. 2012).

Due to the increasing prevalence of NAFLD and the limitations of liver biopsy for diagnosis, there is a strong need for non-invasive tests to accurately detect hepatic steatosis. Magnetic resonance imaging derived proton density fat fraction (MRI-PDFF) has emerged as a leading non-invasive modality for the assessment of hepatic steatosis (Reeder, et al. 2012, Tang, et al. 2013), and as a reliable alternative to the histological assessment of hepatic steatosis in patients with NAFLD (Tang, et al. 2014). However, a wide application of this modality is impaired by its cost and availability. Ultrasound (US) techniques have been proposed since fatty liver is associated with increased US attenuation (Lu, et al. 1999, Gaitini, et al. 2004). In fact, lipid droplets can greatly contribute to energy absorption during US propagation due to their typical dimension in liver tissue (Kanayama, et al. 2013).

US attenuation measurement using controlled attenuation parameter (CAP) (Sasso, et al. 2010, Sasso, et al. 2012, Sasso, et al. 2016) (Echosens, Paris, France) was introduced in 2010 to assess liver steatosis non-invasively. CAP measures the attenuation of the US beam that travels through the liver tissue, usually at a frequency of 3.5 MHz. It is available on the FibroScan (FS) device which concomitantly assesses CAP and liver stiffness using vibration-controlled transient elastography (VCTE) (Sandrin, et al. 2003, Tapper, et al. 2015). The operation of FibroScan does not require special skills in US. CAP can be measured using both M and XL probes. The CAP final results are the median and the interquartile range (IQR) of several (typically 10) manually triggered sequential measurements of US attenuation. CAP is expressed in dB/m and ranges from 100 to 400.

Several US scanner manufacturers have recently introduced alternative methods to assess US attenuation using B-mode US: ATT (Hitachi Ltd, Japan) (Iijima 2018), ATI (Canon Medical Systems, Japan) (Tamaki, et al. 2018, Koizumi, et al. 2019), and UGAP (GE Healthcare, USA) (Fujiwara, et al. 2018, Bende, et al. 2020), UDFF (Siemens Healthineers, Germany) (Labyed and Milkowski 2020). However, US scanners require that the operator be skilled in US as they must select manually a region of interest on the US image to assess the liver tissue. This can be an advantage in the presence of a liver lesion which would not be detected using FS due to the lack of 2D US imaging.

Despite CAP being a good surrogate marker of hepatic steatosis (De Lédinghen, et al. 2014, Cardoso, et al. 2016, De Lédinghen, et al. 2016, De Lédinghen, et al. 2017, Karlas, et al. 2017, Naveau, et al. 2017, Thiele, et al. 2018) and has the ability to monitor the improvement of hepatic steatosis in patients with NAFLD (Paul, et al. 2018, Eddowes, et al. 2019) it has several limitations with its current measurement method. CAP accuracy for detecting fatty liver declines in the presence of high variability (Wong, et al. 2017). In addition, studies on the inter-observer concordance in the CAP values have shown that the mean difference in CAP values between two observers is up to 20 dB/m (Recio, et al. 2013, Ferraioli, et al. 2014). Hence, this

difference should be considered in longitudinal follow-up of patients. Lower performances for detecting fatty liver were reported when the IQR is superior to 40 dB/m (Wong, et al. 2017, Mendes, et al. 2018). Whereas another study shows that CAP variability seems to have no influence on diagnostic performance (Naveau, et al. 2017). The main cause of variability is the sensitivity of CAP to the presence of heterogeneities from blood vessels and nodules in the US signal (Audière, et al. 2013). Furthermore, the distribution of steatosis in the liver may be heterogeneous (Qayyum, et al. 2012, Bannas, et al. 2015). Recent studies (Fujiwara, et al. 2018, Ferraioli, et al. 2019, Ferraioli, et al. 2020) report that US attenuation measurements using B-mode techniques perform significantly better than CAP for steatosis detection with MRI-PDFF as a reference. This increased performance may be attributed to the manual selection of the ROI in the B-mode image which allows the exclusion of structures that may affect the measured values and to the larger 2D ROI which is used to assess ultrasound attenuation. The lack of robustness and precision of the CAP by the standard method is a possible source of suboptimal performances (Petroff, et al. 2021).

We have developed an alternative method for CAP measurement, which uses continuous CAP during the imaging phase of the examination with the FS device that we propose will improve the precision of CAP measurement using FS. The aim of this study was to validate the performances of the new method on tissue-mimicking phantoms and retrospectively in cohorts of patients using MRI-PDFF as a reference.

Material and method

Standard CAP method

CAP measures the US attenuation using US signals collected with the single element US transducer located at tip of the probe of the FS device. Using the standard CAP method, the final CAP results include the median and the IQR (expressed in dB/m) of the individual US attenuation measurements performed during the examination with the FS device. Individual US

attenuation measurements are estimated by processing the US data collected for the shear wave speed measurements, triggered manually by the operator, from which stiffness measurements are derived (Sandrin, et al. 2003). The recommended number of US attenuation measurements is typically 10 since it is recommended that operators perform 10 valid stiffness measurements. Given that a shear wave speed measurement lasts 80 ms, the US attenuation measurements are typically collected during a cumulative duration of less than one second. These individual measurements are distributed over the entire duration of the examination. FS can be used with three different probes (S, M and XL). The standard CAP method is only compatible with M and XL probes (Sasso, et al. 2016). The measurement depths and center frequency with M and XL probes are 25-65 mm and 3.5 MHz, 35-75 mm and 2.5 MHz, respectively. Although the US transducer center frequency is different on the M probe and XL probe, the US attenuation is computed at the same US frequency of 3.5 MHz, leveraging the large bandwidth of US transducers. The lower and upper limits for CAP measurement are 100 dB/m and 400 dB/m, respectively.

Principle of the new method (continuous CAP)

The main difference between the current and the new method is that the new method uses US signals acquired continuously during the imaging phase of the examination with the FS device. For clarity reasons, the new method will therefore be named ‘continuous CAP method’ in this document. The continuous CAP method is as automated as the initial method. The influence on the operation of the device is very limited. Moreover, the proprietary algorithm (Sasso, et al. 2010, Sasso, et al. 2012, Sasso, et al. 2016) used to compute the individual US attenuation measurements using the US signal is identical in both methods. Contrarily to the standard CAP method, the continuous CAP method is compatible with all probes including the S probe (Ferraioli, et al. 2012), which uses a center frequency of 5.0 MHz. The US attenuation is computed at the same US frequency of 3.5 MHz whatever the probe model being used.

Three major improvements are implemented in the continuous CAP method. First, the number of individual US attenuation measurements from which CAP is calculated is higher and corresponds to a larger volume of liver tissue sampled. Second, the US signals are qualified using a dedicated validity criteria. And third, the measurement depths are adapted automatically.

Increased volume sampling

The volume of liver tissue sampled with the standard and continuous CAP methods are schematically represented in figure 1. Using the continuous CAP method, the CAP value is derived from US attenuation measurements which are computed from the US signals acquired continuously in real-time during the imaging phase of the FS examination (i.e., FS imaging mode between stiffness measurements) at a repetition frequency of 20 Hz. At least 200 US attenuation measurements are recommended with the continuous CAP method, which correspond to at least 10 seconds of US acquisition; much larger than the less than 1 second acquisition used with the standard CAP method. Furthermore, during this acquisition time, the liver moves in front of the probe due to breathing with a frequency of approximatively 0.5 Hz, and an amplitude of 20 mm, mainly in the cranio-caudal direction (Bussels, et al. 2003).

Selection of US signals

The selection of US signals used to compute the final CAP value is different in both methods. In the standard CAP method, US signals are selected based on the validity of the shear wave propagation induced when the operator presses on the probe button. In the continuous CAP method, US signals are selected based on the US characteristics of the signals. The selection of US signals is performed automatically using the Liver Targeting Tool (LTT) (Audière, et al. 2013), which assesses the absence of heterogeneities in the US signal. LTT is displayed in real-time on the screen of the FS during the examination to assist the operators in finding an optimal measurement site.

Measurement depths automated adjustment

The continuous CAP method includes an automated adaptation of the measurements depths based on the probe to liver capsule distance (PCD) (Audière, et al. 2010). The purpose is to avoid biases of US attenuation measurements in the presence of subcutaneous tissues in the region of measurements. Several depth ranges are available depending on the probe model: 25-65 mm or 30-70 mm with the M probe, 35-75 mm, 40-80 mm or 45-85 mm with the XL probe. With the S probe, depth ranges are selected manually at the beginning of the exam and correspond to the stiffness measurement depths (S1: 15-40 mm, S2: 20-50 mm).

Examination outputs

Given the large number of individual measurements collected with the continuous CAP method, a normal distribution of measurements is observed. The final CAP results are expressed as the mean and standard deviation (SD).

Test on tissue-mimicking phantoms

Tissue-mimicking phantoms characteristics

The standard CAP and continuous CAP methods were tested on seven custom reference tissue-mimicking phantoms (Gammex INC, Middleton, WI, USA), which US attenuations are 95, 142, 207, 249, 339, 403 and 475 dB/m, with an uncertainty ± 20 dB/m. Reference US attenuation values were measured at the Wisconsin Institute of Medical Research (Madison, WI 53705, USA) for each phantom using a sample of each batch material. A standard narrowband through-transmission substitution technique (Madsen, et al. 1982) was used.

Test method

The continuous CAP method was evaluated with S, M and XL probes while the standard CAP method was only evaluated with M and XL probes given that the S probe is not compatible. US acquisitions measurements were performed with a FS device acquisition platform connected to a standard computer running Matlab (Mathworks, Natick, MA, USA). The shear wave

generation was disabled since the reference US attenuation phantoms were too stiff to obtain valid stiffness measurements. Each set of measurements consisted in scanning a phantom by moving the probe in the center (20 x 20 mm^2) of the phantom surface. A motorized linear translation stage (Newport Corporation, Irvine, CA, USA) was used to move the probes at the surface of the phantom, with a displacement speed of 20 mm/s. Acquisitions for the assessment of the continuous CAP method were performed while the probe was moving at the surface of the phantom to mimic the liver movement during the FS imaging mode, allowing to achieve 200 US attenuation measurements. Acquisitions for the assessment of the standard CAP method were performed with a step by step displacement of the probe at the surface of the phantom to mimic the acquisition of US signals during the FS sequential stiffness measurements. Ten individual measurements were performed at 10 different locations within the same region of interest used with the continuous CAP method. Acquisitions for both methods were performed at the same depths. Due to the large distribution of the reference US attenuation of tissue-mimicking phantoms, the lower and upper limits for CAP measurement were set to 50 dB/m and 500 dB/m, respectively.

Statistical analysis

The Shapiro-Wilk test was used to assess the normal distribution of the measurements performed with both methods. For comparison purposes, the standard CAP results were expressed as the mean (instead of median for the standard CAP method) of all performed measurements. The CAP precision is expressed as the SD. The significance of the precision difference between the two methods is achieved through a Student's-test.

The intra-class coefficient (ICC) was used to assess the agreement between the two methods and the reproducibility on phantoms, as suggested in (Raunig, et al. 2015). Two other probes of each type were used to estimate the reproducibility of both methods. Agreement was classified as poor (ICC = 0.00-0.20), fair to good (ICC = 0.40-0.75) or excellent (ICC > 0.75) (Fleiss, et al. 2013).

In vivo studies

The comparison between both CAP methods was performed using clinical data collected during two different studies (study cohorts A and B). MRI-PDFF was used as a reference to identify the ability of both CAP methods to identify patients with a MRI-PDFF of more than 5%. The study protocols conformed to the ethical guidelines of the 1975 Declaration of Helsinki and was approved by the local Ethic committee. Patients were enrolled after written informed consent was obtained. For both study cohorts, CAP measurements were performed with a FibroScan 502 Touch configured to record the raw US radio-frequency signals collected during the whole FS examinations. The operators were following the training requirements relative to the standard measurements of liver stiffness by VCTE and CAP. The continuous CAP method was evaluated retrospectively by reprocessing the raw data recorded in examination files of the standard CAP method.

Study cohort A

Patients referred for a routine liver screening with no prior history of liver disease or alcohol abuse were offered to participate in this prospective prevalence study. All patients who underwent CAP and MRI-PDFF examinations at the Brooke Army Medical Center (San Antonio, Texas, USA) between January 2016 and December 2016 were eligible. MRI-PDFF results were reprocessed with Liver MultiScan IDEAL algorithm (Hardy and Mcpherson 2017) (liver MultiScan™, Perspectum Diagnostics, Oxford, England), which assesses hepatic steatosis, fibrosis and iron content. Region of interest (ROI) was positioned by the clinician on the MRI-PDFF parametric image, taking the most representative area. This area is positioned without taking into account the position of the FS measurement.

A total of 201 consecutive patients fulfilled the inclusion criteria (male and female patients, age 18 to 80), and consisted of retired and active military personnel and their dependents. Among them, 74 were excluded because the MRI-PDFF could not be performed and 14 because the

delay between FS and MRI-PDFF examinations was superior to 100 days. Finally, the study A included 113 patients.

Study cohort B

Patients referred for a liver MRI examination were offered participation in a prospective prevalence study. All patients who underwent CAP and MRI-PDFF examinations at the ACRIM-Polyclinique Saint-Côme (Compiègne, France) between February 2017 and October 2018 were eligible. MRI-PDFF ROI in liver were placed at nearly the same location as the ROI of the FS examination (Bensamoun, et al. 2008, Ternifi, et al. 2018)

A total of 90 consecutive patients fulfilled the inclusion criteria (male and female patients, age 18 to 80). Among them, five were excluded because the CAP files with raw US data were unusable (corrupted files) and two patients because the matching between FS and MRI examinations was not possible. One patient was also excluded because MRI-PDFF was not performed. Finally, the study B included 82 patients.

The two study cohorts were not pulled as they involved different MRI devices associated with different algorithms for the reconstruction of MRI-PDFF maps. Furthermore, the ROI placements were performed by two different teams, with two different techniques as explained above.

Magnetic Resonance Imaging

MRI-PDFF magnetic resonance imaging-based phenotyping was performed using 1.5T MRI devices (Avanto, Siemens, and Signa HDx, General Electric). Patients were in the supine position. MRI-PDFF results were estimated using the Dixon 3 points method (Ma 2008) in both studies.

Statistical analysis

CAP results were expressed as the median and the mean of all valid measurements for the standard CAP method and the continuous CAP method, respectively. SD was used to assess the

precision of both methods to ease the comparison. The significance of the precision difference between the two methods is achieved through a Student's-test.

The ICC were used to assess the agreement between the two methods. A Bland Altman analysis was used to determine the bias between the two methods.

Data collected in vivo were used to assess the performance of both CAP methods versus MRI-PDFF. Pearson's rank correlations were used to evaluate the relationship between CAP values and log MRI-PDFF. Correlation obtained with both CAP methods were compared using the Hittner's test. The test is significant if the p-value is <0.05. The performance of both CAP methods for identifying patients with hepatic steatosis defined by MRI-PDFF of more than 5% was assessed using a Receiver Operating Characteristic (ROC) analysis. The diagnostic performance was evaluated in terms of area under the receiver operating curve (AUROC). AUROC obtained with both CAP methods were compared using the Delong test (difference test and non-inferiority test with a 0.02 margin). The test is significant if the p-value is <0.05. CAP cut-off values were estimated by maximizing sensitivity and specificity (Youden's index). A linear fit was performed between CAP (in dB/m) and the logarithmic transformation of MRI-PDFF (in percentage). All statistical analyses were performed using the R software (The R Foundation for Statistical Computing, Vienna, Austria) and the graphics, stats, pROC, ggplot2, IRR, BlandAltmanLeh and RVAideMemoire packages.

Results

Validation on tissue-mimicking phantoms

We assessed the two CAP methods with seven tissue-mimicking phantoms. The comparison and precision of both CAP methods versus reference US attenuations are presented in figure 2. The precision of both CAP methods for each scan is represented by an error bar (±SD). The results of the linear regressions between CAP and reference US attenuations are provided on each graph. The relationship is closer to identity with the continuous CAP method than with

the standard CAP. As shown in figure 3, the precision (in term of SD) was improved by 57% and 63% for M and XL probes, respectively. The ICC between the standard and continuous CAP methods was 0.996 [0.978; 0.999] and 0.988 [0.935; 0.998], with the M probe and XL probe respectively, showing excellent agreement. In terms of reproducibility, the ICC for both methods are all above 0.98.

In vivo validation

Patients and examinations characteristics

As described above, two study cohorts were formed of 113 patients for cohort A and 82 patients for cohort B. The characteristics of the two study cohorts are provided in table 1. For studies A and B, respectively 83% and 94% of CAP measurements were performed at the same depth for both methods. In study A, 88% of FS examinations were performed by the same expert operator. In study B, FS examinations were equitably distributed between two novice operators.

Comparison versus MRI-PDFF

The comparison of both CAP methods versus MRI-PDFF in both study cohorts is given in table 2. The relationships between MRI-PDFF and CAP are shown figure 4. ROC curves for a MRI-PDFF $\geq$ 5% are shown figure 5.

Agreement between standard and continuous methods, bias, precisions

The ICC between the standard and continuous CAP methods was 0.901 and 0.940 for study cohort A and B, respectively. A Bland Altman analysis is presented in figure 6. Compared to the standard method, the CAP continuous method is on average 8.6 dB/m and 5.6 dB/m lower for study cohort A and B, respectively.

The precisions of both CAP methods are presented in figure 7. Box-and-whisker plots were used to appraise the precision of both CAP methods. In study cohort A, the precision was improved by 41% and 33% using the continuous CAP method with the M probe and XL probe,

respectively. In study cohort B, the precision was improved by 38% and 22% using the continuous CAP method with the M probe and XL probe, respectively.

Discussion

This study demonstrates that the precision of CAP measurement can be improved using the new continuous CAP method. The main difference between the standard and the continuous CAP method was the collection and selection of the US signals used to compute the US attenuation. The continuous CAP method relies on the collection of US signals collected during the imaging mode of the examination with a FS device. Furthermore, only US signals of sufficient quality in terms of homogeneity are automatically selected for computation. The performances of the standard and new methods were studied in phantoms as well as in vivo.

The tests on homogeneous tissue-mimicking phantoms of known reference US attenuations demonstrated that both the standard and continuous CAP methods are accurate although the precision with the continuous CAP method was improved by 57% and 63% for M probe and XL probe, respectively. ICC between the two methods and reproducibility tests showed a perfect agreement. The improved precision of CAP measurements using the continuous CAP method was also observed in vivo in the two study cohorts. The precision of CAP was on average improved by 34% with the new method.

Given that US signals obtained on tissue-mimicking phantoms are free of artefacts, the improved precision on phantoms may be attributed only to the larger number of US attenuation measurements collected with the new method.

The improvement of precision with the continuous CAP method is obtained by collecting the US signals during the imaging mode of the examination with the FS device instead of relying on the US signals collected for liver stiffness measurements. In study cohort A and study cohort B, the number of US attenuation measurements collected during the imaging mode and used for CAP measurement is on average 900 and 1555, respectively. These numbers are much

higher than the 10 US attenuation values usually obtained with the standard CAP method. Furthermore, given that these values are collected at a maximum pulse-repetition frequency of 20 Hz, they translate into equivalent durations of 45 seconds and 778 seconds, respectively. These durations are much higher than the equivalent duration using the standard CAP method, which is about one second. The longer acquisition time associated with liver movement due to breathing significantly increases the volume of liver tissue sampled with the new method and therefore the spatial averaging. Consequently, the precision of the final CAP value with the continuous CAP method is better than with the standard method. Although different US signals are used for the assessment of CAP and liver stiffness measurements using the continuous CAP method. Both values still reflect the same portion of the liver as they are acquired during the same examination, which combines imaging sequences during which US attenuation values are collected and elastography measurement sequences during which shear wave speed and stiffness values are measured.

The continuous CAP method demonstrated superior performances (although not significantly) in terms of AUROCs and correlation with MRI-PDFF in both study cohorts, which suggests a diagnostic performance at least as good as the standard CAP method. The Delong test with a 0.02 AUROC margin demonstrated a significant non-inferiority of the continuous CAP method when compared to standard CAP method. This improvement may be attributed to the improved precision and the enhanced selection of US signals used in both methods. As a matter of fact, in the standard CAP method the selection of US signals is based on the validity of stiffness measurement which may be suboptimal. Indeed, the US attenuation estimate is influenced by the presence of heterogeneities in the US signal which may not affect the shear wave propagation map and the associated shear wave speed assessment. The presence of subcutaneous tissues (fat, muscle, etc.) or blood vessels within the ROI (Shen, et al. 2015) usually result in hyperechogeneic artefacts in the US signals, which may - depending on their position in the ROI - give overestimations or underestimations and associated false positive or

false negative. The enhanced selection of US signals based on their US characteristics may contribute to decreases in the influence of US artefacts.

The ICC between the two CAP methods showed a perfect in vivo agreement, which confirms that the two methods measure the same US attenuation parameter. The Bland Altman results show that the new CAP method is on average slightly lower than CAP with standard method. The automatic ROI selection according to the subcutaneous thickness and the selection of the valid US signals may explain this trend.

The linear regression fits between the standard and the new method versus MRI-PDFF are slightly different in the two study cohorts. This variation may be attributed to differences in the MRI-PDFF measurement methods used in the two study cohorts and to the significantly different BMI distributions in the two study cohorts. The good agreement found between the standard CAP method and the continuous CAP method is supported by using the exact same core algorithm to compute the individual US attenuation values. A good agreement between both methods is important to ensure that the published CAP cut-offs obtained with the standard CAP method can be used with the continuous CAP method. Interestingly, as the relationship between CAP expressed in dB/m and MRI-PDFF expressed in percentage is logarithmic, a relative decrease in MRI-PDFF would result in an absolute decrease in CAP value. For an example, given the coefficients obtained using the regression (table 2), a relative decrease of 30% in MRI-PDFF corresponds to a decrease of 14 to 18 dB/m in CAP value.

A limitation of this study is that the new method was evaluated retrospectively by reprocessing the raw data recorded during examinations which were performed using a FS device with the standard CAP method. Future studies will help assess the performances of the new method when the operator is provided with the actual real-time information relative to the collection of US attenuation measurements. Another limitation is the use of MRI-PDFF as a reference instead of histopathology. Indeed, MRI-PDFF results may be influenced by several factors including the MRI device model, the calculation method (Liver MultiScan for study cohort A and clinical

procedure for study cohort B), the size of the ROI and the manual selection of the MRI-PDFF ROI by the radiologist (Campo, et al. 2017). Some studies assessed the accuracy and reproducibility of MRI-PDFF for multivendor MRI on phantoms (Hernando, et al. 2017, Hayashi, et al. 2018). With a standard reconstruction algorithm, the relative error is inversely proportional to the true fat fraction of phantom. The error is about 20% for low fat fraction and about 5% for high fat fraction. For study cohort A, the delay between FS examination and MRI-PDFF examination can reach several weeks and may compromise the relevance of the results because of the progression of steatosis. With the uncertainties on the etiology of the steatosis, these MRI-PDFF limitations could explain the inconsistency of MRI-PDFF distribution between the two study cohorts. Lastly, in this study no artificial body wall between the FS and the phantom material has been included as we used a single element US transducer with a small aperture of approximatively 1 cm^2. However, it will be of interest to analyze the impact of the artificial body wall on the CAP measurements.

Conclusion

In this study, a new method for CAP measurement was successfully validated on US attenuation reference phantoms and retrospectively on in vivo data from two study cohorts. The continuous CAP method significantly improves the precision of US attenuation assessment. Furthermore, the new method demonstrated higher performances in terms of hepatic steatosis quantification when using MRI-PDFF as a reference and a better correlation with MRI-PDFF. The new method is implemented in FS devices with only minor changes in the operation of the examination. The differences include the introduction of a specific gage to reflect the number of US attenuation measurements, and the use of the mean and the SD instead of median and IQR, respectively. A perfect agreement was found between both methods, indicating that the cut-offs defined for CAP in the literature are applicable to CAP measurements performed with the new method. CAP measured using the continuous CAP method is a promising tool and a reliable alternative or complement the standard CAP method for diagnosing and monitoring

hepatic steatosis during longitudinal follow-up of patients with chronic liver disease. These preliminary results should be confirmed in a larger prospective study.

Acknowledgements

The authors are very grateful to the research biomedical engineer Jennifer Whitehead, as well as the expert pathologist Dr. Angelo H. Paredes, from Brooke army medical center.

The authors would like to thank Laura A. Kehoe for her help in improving the English of this paper.

Conflicts of interest

Stéphane Audière, Aymeric Labourdette, Céline Fournier, Laurent Sandrin and Véronique Miette are Echosens employees. Stephen A. Harrison is a consultant of Echosens. Redouane Ternifi and Salem Boussida received support from Echosens. All other authors declare no conflicts of interest.

Reference List

Audière S, Charbit M, Angelini ED, Oudry J, Sandrin L. 2010 Measurement of the skin-liver capsule distance on ultrasound RF data for 1D transient elastography. *International Conference on Medical Image Computing and Computer-Assisted Intervention*: Springer, 34-41.

Audière S, Clet M, Sasso M, Sandrin L, Miette V. 2013 Influence of heterogeneities on ultrasound attenuation for liver steatosis evaluation (CAP™): relevance of a liver guidance tool. *IEEE International Ultrasonics Symposium (IUS)*: IEEE, 401-04.

Bannas P, Kramer H, Hernando D, Agni R, Cunningham AM, Mandal R, Motosugi U, Sharma SD, Munoz del Rio A, Fernandez L, Reeder SB. Quantitative magnetic resonance imaging of hepatic steatosis: Validation in ex vivo human livers. Hepatology 2015;62:1444-55.

Bende F, Sporea I, Șirli R, Bâldea V, Lazăr A, Lupușoru R, Fofiu R, Popescu A. Ultrasound-Guided Attenuation Parameter (UGAP) for the quantification of liver steatosis using the Controlled Attenuation Parameter (CAP) as the reference method. Medical Ultrasonography 2020;23:7-14.

Bensamoun SF, Wang L, Robert L, Charleux F, Latrive JP, Ho Ba Tho MC. Measurement of liver stiffness with two imaging techniques: magnetic resonance elastography and ultrasound elastometry. Journal of Magnetic Resonance Imaging: An Official Journal of the International Society for Magnetic Resonance in Medicine 2008;28:1287-92.

Bravo AA, Sheth SG, Chopra S. Liver biopsy. New England Journal of Medicine 2001;344:495-500.

Bussels B, Goethals L, Feron M, Bielen D, Dymarkowski S, Suetens P, Haustermans K. Respiration-induced movement of the upper abdominal organs: a pitfall for the three-dimensional conformal radiation treatment of pancreatic cancer. Radiother Oncol 2003;68:69-74.

Campo CA, Hernando D, Schubert T, Bookwalter CA, Pay AJV, Reeder SB. Standardized approach for ROI-based measurements of proton density fat fraction and R2* in the liver. American Journal of Roentgenology 2017;209:592-603.

Cardoso AC, Beaugrand M, de Ledinghen V, Douvin C, Poupon R, Trinchet J-C, Ziol M, Bedossa P, Marcellin P. Diagnostic performance of controlled attenuation parameter for predicting steatosis grade in chronic hepatitis B. Annals of hepatology 2016;14:826-36.

de Lédinghen V, Hiriart J-B, Vergniol J, Merrouche W, Bedossa P, Paradis V. Controlled attenuation parameter (CAP) with the XL probe of the Fibroscan®: a comparative study with the M probe and liver biopsy. Digestive diseases and sciences 2017;62:2569-77.

de Lédinghen V, Vergniol J, Capdepont M, Chermak F, Hiriart J-B, Cassinotto C, Merrouche W, Foucher J. Controlled attenuation parameter (CAP) for the diagnosis of steatosis: a prospective study of 5323 examinations. Journal of hepatology 2014;60:1026-31.

de Lédinghen V, Wong GLH, Vergniol J, Chan HLY, Hiriart JB, Chan AWH, Chermak F, Choi PCL, Foucher J, Chan CKM. Controlled attenuation parameter for the diagnosis of steatosis in non-alcoholic fatty liver disease. Journal of gastroenterology and hepatology 2016;31:848-55.

Eddowes PJ, Sasso M, Allison M, Tsochatzis E, Anstee QM, Sheridan D, Guha IN, Cobbold JF, Deeks JJ, Paradis V. Accuracy of FibroScan controlled attenuation parameter and liver stiffness measurement in assessing steatosis and fibrosis in patients with nonalcoholic fatty liver disease. Gastroenterology 2019;156:1717-30.

Elizabeth LY, Golshan S, Harlow KE, Angeles JE, Durelle J, Goyal NP, Newton KP, Sawh MC, Hooker J, Sy EZ. Prevalence of nonalcoholic fatty liver disease in children with obesity. The Journal of pediatrics 2019;207:64-70.

Ferraioli G, Lissandrin R, Zicchetti M, Filice C. Assessment of liver stiffness with transient elastography by using S and M probes in healthy children. European journal of pediatrics 2012;171:1415-15.

Ferraioli G, Maiocchi L, Raciti MV, Tinelli C, De Silvestri A, Nichetti M, De Cata P, Rondanelli M, Chiovato L, Calliada F. Detection of liver steatosis with a novel ultrasound-based technique: a pilot study using MRI-derived proton density fat fraction as the gold standard. Clinical and translational gastroenterology 2019;10:1-8.

Ferraioli G, Maiocchi L, Savietto G, Tinelli C, Nichetti M, Rondanelli M, Calliada F, Preda L, Filice C. Performance of the Attenuation Imaging Technology in the Detection of Liver Steatosis. Journal of Ultrasound in Medicine 2020;40:1325-32.

Ferraioli G, Tinelli C, Lissandrin R, Zicchetti M, Rondanelli M, Perani G, Bernuzzi S, Salvaneschi L, Filice C. Interobserver reproducibility of the controlled attenuation parameter (CAP) for quantifying liver steatosis. Hepatology international 2014;8:576-81.

Fleiss JL, Levin B, Paik MC. Statistical methods for rates and proportions: John Wiley & Sons, 2013.

Fujiwara Y, Kuroda H, Abe T, Ishida K, Oguri T, Noguchi S, Sugai T, Kamiyama N, Takikawa Y. The B-Mode Image-Guided Ultrasound Attenuation Parameter Accurately Detects Hepatic Steatosis in Chronic Liver Disease. Ultrasound Med Biol 2018;44:2223-32.

Gaitini D, Baruch Y, Ghersin E, Veitsman E, Kerner H, Shalem B, Yaniv G, Sarfaty C, Azhari H. Feasibility study of ultrasonic fatty liver biopsy: texture vs. attenuation and backscatter. Ultrasound Med Biol 2004;30:1321-7.

Hardy T, McPherson S. Imaging-based assessment of steatosis, inflammation and fibrosis in NAFLD. Current Hepatology Reports 2017;16:298-307.

Harrison SA, Gawrieh S, Roberts K, Lisanti CJ, Schwope RB, Cebe KM, Paradis V, Bedossa P, Aldridge Whitehead JM, Labourdette A, Miette V, Neubauer S, Fournier C, Paredes AH, Alkhouri N. Prospective evaluation of the prevalence of non-alcoholic fatty liver disease and steatohepatitis in a large middle-aged US cohort. J Hepatol 2021.

Hayashi T, Fukuzawa K, Yamazaki H, Konno T, Miyati T, Kotoku Ji, Oba H, Kondo H, Toyoda K, Saitoh S. Multicenter, multivendor phantom study to validate proton density fat fraction and T2* values calculated using vendor-provided 6-point DIXON methods. Clinical imaging 2018;51:38-42.

Hernando D, Sharma SD, Aliyari Ghasabeh M, Alvis BD, Arora SS, Hamilton G, Pan L, Shaffer JM, Sofue K, Szeverenyi NM. Multisite, multivendor validation of the accuracy and reproducibility of proton- density fat- fraction quantification at 1.5 T and 3T using a fat–water phantom. Magnetic resonance in medicine 2017;77:1516-24.

Iijima H. 2018 Assessment of non-alcoholic fatty liver disease with Attenuation Imaging (ATI). *VISIONS n°30*: CANON MEDICAL SYSTEMS // ULEU170064.

Kanayama Y, Kamiyama N, Maruyama K, Sumino Y. Real-time ultrasound attenuation imaging of diffuse fatty liver disease. Ultrasound Med Biol 2013;39:692-705.

Karlas T, Petroff D, Sasso M, Fan JG, Mi YQ, de Ledinghen V, Kumar M, Lupsor-Platon M, Han KH, Cardoso AC, Ferraioli G, Chan WK, Wong VW, Myers RP, Chayama K, Friedrich-Rust M, Beaugrand M, Shen F, Hiriart JB, Sarin SK, Badea R, Jung KS, Marcellin P, Filice C, Mahadeva S, Wong GL, Crotty P, Masaki K, Bojunga J, Bedossa P, Keim V, Wiegand J. Individual patient data meta-analysis of controlled attenuation parameter (CAP) technology for assessing steatosis. J Hepatol 2017;66:1022-30.

Koizumi Y, Hirooka M, Tamaki N, Yada N, Nakashima O, Izumi N, Kudo M, Hiasa Y. New diagnostic technique to evaluate hepatic steatosis using the attenuation coefficient on ultrasound B mode. PloS one 2019;14:e0221548.

Labyed Y, Milkowski A. Novel Method for Ultrasound- Derived Fat Fraction Using an Integrated Phantom. Journal of Ultrasound in Medicine 2020;39:2427-38.

Lu ZF, Zagzebski JA, Lee FT. Ultrasound backscatter and attenuation in human liver with diffuse disease. Ultrasound Med Biol 1999;25:1047-54.

Ma J. Dixon techniques for water and fat imaging. J Magn Reson Imaging 2008;28:543-58.

Madsen EL, Zagzebski JA, Frank GR. Oil-in-gelatin dispersions for use as ultrasonically tissue-mimicking materials. Ultrasound in Medicine and Biology 1982;8:277-87.

Mendes LC, Ferreira PA, Miotto N, Zanaga L, Lazarini MS, Goncales ESL, Pedro MN, Goncales FLJ, Stucchi RSB, Vigani AG. Controlled attenuation parameter for steatosis grading in chronic hepatitis C compared with digital morphometric analysis of liver biopsy: impact of individual elastography measurement quality. Eur J Gastroenterol Hepatol 2018;30:959-66.

Naveau S, Voican CS, Lebrun A, Gaillard M, Lamouri K, Njike-Nakseu M, Courie R, Tranchart H, Balian A, Prevot S, Dagher I, Perlemuter G. Controlled attenuation parameter for diagnosing

steatosis in bariatric surgery candidates with suspected nonalcoholic fatty liver disease. Eur J Gastroenterol Hepatol 2017;29:1022-30.

Paul J, Venugopal RV, Peter L, Shetty KNK, Shetti MP. Measurement of Controlled Attenuation Parameter: A Surrogate Marker of Hepatic Steatosis in Patients of Nonalcoholic Fatty Liver Disease on Lifestyle Modification - a Prospective Follow-up Study. Arq Gastroenterol 2018;55:7-13.

Petroff D, Blank V, Newsome PN, Voican CS, Thiele M, de Lédinghen V, Baumeler S, Chan WK, Perlemuter G, Cardoso A-C. Assessment of hepatic steatosis by controlled attenuation parameter using the M and XL probes: an individual patient data meta-analysis. The Lancet Gastroenterology & Hepatology 2021;6:185-98.

Qayyum A, Nystrom M, Noworolski SM, Chu P, Mohanty A, Merriman R. MRI steatosis grading: development and initial validation of a color mapping system. AJR Am J Roentgenol 2012;198:582-8.

Ratziu V, Charlotte F, Heurtier A, Gombert S, Giral P, Bruckert E, Grimaldi A, Capron F, Poynard T, Group LS. Sampling variability of liver biopsy in nonalcoholic fatty liver disease. Gastroenterology 2005;128:1898-906.

Raunig DL, McShane LM, Pennello G, Gatsonis C, Carson PL, Voyvodic JT, Wahl RL, Kurland BF, Schwarz AJ, Gonen M, Zahlmann G, Kondratovich MV, O'Donnell K, Petrick N, Cole PE, Garra B, Sullivan DC, Group QTPW. Quantitative imaging biomarkers: a review of statistical methods for technical performance assessment. Stat Methods Med Res 2015;24:27-67.

Recio E, Cifuentes C, Macías J, Mira JA, Parra-Sánchez M, Rivero-Juárez A, Almeida C, Pineda JA, Neukam K. Interobserver concordance in controlled attenuation parameter measurement, a novel tool for the assessment of hepatic steatosis on the basis of transient elastography. European Journal of Gastroenterology & Hepatology 2013;25:905-11.

Reeder SB, Hu HH, Sirlin CB. Proton density fat-fraction: a standardized MR-based biomarker of tissue fat concentration. J Magn Reson Imaging 2012;36:1011-4.

Sandrin L, Fourquet B, Hasquenoph JM, Yon S, Fournier C, Mal F, Christidis C, Ziol M, Poulet B, Kazemi F, Beaugrand M, Palau R. Transient elastography: a new noninvasive method for assessment of hepatic fibrosis. Ultrasound Med Biol 2003;29:1705-13.

Sasso M, Audiere S, Kemgang A, Gaouar F, Corpechot C, Chazouilleres O, Fournier C, Golsztejn O, Prince S, Menu Y, Sandrin L, Miette V. Liver Steatosis Assessed by Controlled Attenuation Parameter (CAP) Measured with the XL Probe of the FibroScan: A Pilot Study Assessing Diagnostic Accuracy. Ultrasound Med Biol 2016;42:92-103.

Sasso M, Beaugrand M, De Ledinghen V, Douvin C, Marcellin P, Poupon R, Sandrin L, Miette V. Controlled attenuation parameter (CAP): a novel VCTE™ guided ultrasonic attenuation measurement for the evaluation of hepatic steatosis: preliminary study and validation in a cohort of patients with chronic liver disease from various causes. Ultrasound in medicine & biology 2010;36:1825-35.

Sasso M, Miette V, Sandrin L, Beaugrand M. The controlled attenuation parameter (CAP): A novel tool for the non-invasive evaluation of steatosis using Fibroscan®. Clinics and research in hepatology and gastroenterology 2012;36:13-20.

Shahin Merat M, Rasoul Sotoudehmanesh M, Mehdi Nouraie M, Masoumeh Peikan-Heirati M, Sadaf G, Reza Malekzadeh M, Sotoudeh M. Sampling error in histopathology findings of nonalcoholic fatty liver disease: a post mortem liver histology study. Archives of Iranian medicine 2012;15:418.

Shen F, Zheng RD, Shi JP, Mi YQ, Chen GF, Hu X, Liu YG, Wang XY, Pan Q, Chen GY, Chen JN, Xu L, Zhang RN, Xu LM, Fan JG. Impact of skin capsular distance on the performance of controlled attenuation parameter in patients with chronic liver disease. Liver Int 2015;35:2392-400.

Tamaki N, Koizumi Y, Hirooka M, Yada N, Takada H, Nakashima O, Kudo M, Hiasa Y, Izumi N. Novel quantitative assessment system of liver steatosis using a newly developed attenuation measurement method. Hepatology Research 2018;48:812-28.

Tang A, Desai A, Hamilton G, Wolfson T, Gamst A, Lam J, Clark L, Hooker J, Chavez T, Ang BD. Accuracy of MR imaging–estimated proton density fat fraction for classification of dichotomized histologic steatosis grades in nonalcoholic fatty liver disease. Radiology 2014;274:416-25.

Tang A, Tan J, Sun M, Hamilton G, Bydder M, Wolfson T, Gamst AC, Middleton M, Brunt EM, Loomba R, Lavine JE, Schwimmer JB, Sirlin CB. Nonalcoholic fatty liver disease: MR imaging of liver proton density fat fraction to assess hepatic steatosis. Radiology 2013;267:422-31.

Tapper EB, Castera L, Afdhal NH. FibroScan (vibration-controlled transient elastography): where does it stand in the United States practice. Clinical Gastroenterology and Hepatology 2015;13:27-36.

Ternifi R, Pouletaut P, Sasso M, Miette V, Charleux F, Bensamoun S. Improvements of Liver MR Imaging Clinical Protocols to Simultaneously Quantify Steatosis and Iron Overload. IRBM 2018;39:219-25.

Thiele M, Rausch V, Fluhr G, Kjaergaard M, Piecha F, Mueller J, Straub BK, Lupsor-Platon M, De-Ledinghen V, Seitz HK, Detlefsen S, Madsen B, Krag A, Mueller S. Controlled attenuation parameter and alcoholic hepatic steatosis: Diagnostic accuracy and role of alcohol detoxification. J Hepatol 2018;68:1025-32.

Wong VW, Petta S, Hiriart JB, Camma C, Wong GL, Marra F, Vergniol J, Chan AW, Tuttolomondo A, Merrouche W, Chan HL, Le Bail B, Arena U, Craxi A, de Ledinghen V. Validity criteria for the diagnosis of fatty liver by M probe-based controlled attenuation parameter. J Hepatol 2017;67:577-84.

Younossi ZM, Koenig AB, Abdelatif D, Fazel Y, Henry L, Wymer M. Global epidemiology of nonalcoholic fatty liver disease—meta- analytic assessment of prevalence, incidence, and outcomes. Hepatology 2016;64:73-84.

Figure Caption list

Figure 1. Schematic representation of liver tissues sampled with (a) the standard CAP method and (b) the continuous CAP method. PCD = Probe to liver Capsule Distance.

Figure 2. Comparison of CAP measurements obtained with both the standard and continuous CAP methods with reference attenuation values on seven tissue-mimicking phantoms. The precision is represented by an error bar (±SD). Dash lines and equations represent the linear fit between the reference attenuation and the CAP measurement. R^2 is the coefficient of determination of the fit.

Figure 3. Distribution of CAP precision (SD) obtained with the standard and continuous CAP methods using the M, S and XL probes. The significant test of the precision difference is performed with a t-test (*** = $p < 0.001$). In the box plots, the boundary of the box closest to zero indicates the 25^{th} percentile, a black line within the box marks the median, and the boundary of the box farthest from zero indicates the 75^{th} percentile. The length of the vertical lines above and below the box is 1.5 times the IQR. Outlier: any patient result lying outside the upper or lower whiskers.

Figure 4. CAP versus MRI-PDFF for study cohort A (a) and study cohort B (b) using the standard and continuous CAP methods. Dash lines represent the linear fit between logarithmic PDFF and CAP. R^2 is the coefficient of determination of the fit. Pearson values are the results of the Pearson correlations.

Figure 5. Receiver operating curves (ROC) analysis of CAP for the detection of patients with hepatic steatosis defined by MRI-PDFF $\geq$ 5%. Standard CAP method (dash lines) and continuous CAP method (plain line) for study cohort A (a) and study cohort B (b).

Figure 6. Bland Altman plot of differences between standard CAP method and continuous CAP method measurements vs. the mean of the two measurements. For study cohort A (a) and study

cohort B (b), the mean difference (8.6 dB/m, 5.6 dB/m) and the lower and upper limits of agreement (-32.9 and 50.1 dB/m, -31.9 and 43.1 dB/m) are represented as dashed lines.

Figure 7. Distribution of CAP precision obtained with the standard and continuous CAP methods using the M and XL probes for study cohort A (a) and study cohort B (b). The IQR of the standard CAP method provided for indication only. The significant test of the precision improvement is performed with a t-test (** $p < 0.01$, **** $p < 0.0001$). In the box plots, the boundary of the box closest to zero indicates the 25^{th} percentile, a black line within the box marks the median, and the boundary of the box farthest from zero indicates the 75^{th} percentile. The length of the vertical lines above and below the box is 1.5 times the IQR. Outlier: any patient result lying outside the upper or lower whiskers.

Table 1. Characteristics of the two study cohorts.

Study cohort	A	B
Patients		
Number of patients	113	82
Male	44%	56%
Age **Mean ± SD (years)**	53 ± 8	55 ± 19
BMI **Mean ± SD (kg/m²)**	30 ± 5	27 ± 5
Normal weight / Overweight / Obese	16% / 38% / 46%	38% / 30% / 21%
FS examinations		
M probe / XL probe	69% / 31%	73% / 27%
At least 10 valid measurements	100%	96%
At least recommended number of US attenuation measurements for continuous CAP method	94%	100%
PCD M & XL probes **Mean ± SD (mm)**	M: 17.4 ± 2.9 XL: 24.0 ± 4.4	M: 16.1 ± 2.9 XL: 21.8 ± 2.6
Standard CAP method values **Mean ± SD (dB/m)**	275.3 ± 52.3	264.9 ± 57.9
Continuous CAP method values **Mean ± SD (dB/m)**	266.8 ± 49.3	259.6 ± 56.4
Number of US attenuation measurements Standard CAP method **Mean ± SD**	10.2 ± 0.8	11.0 ± 3.4
Number of US attenuation measurements Continuous CAP method **Mean ± SD**	900 ± 599	1555 ± 834
MRI-PDFF examinations		
MRI-PDFF **Median [IQR] (%)**	2.7 [5.1]	5.83 [9.7]
Delay between MRI-PDFF & FS **Median [IQR] (days)**	22 [30]	0 [0]

SD = standard deviation; PCD = probe to liver capsule distance; US = ultrasound; MRI-PDFF = magnetic resonance imaging - proton density fat fraction; FS = FibroScan; IQR = interquartile range.

Table 2. Comparison of both CAP methods versus MRI-PDFF in the two study cohorts.

Study cohort		A	B
Pearson correlations CAP vs log10(PDFF)	*Standard CAP method*	0.71 [0.60-0.79]	0.71 [0.58-0.80]
	Continuous CAP method	0.74 [0.65-0.81]	0.76 [0.66-0.84]
	Hittner test p-value	0.22	0.02
Regression CAP = a x log10(PDFF) + b	*Standard CAP method*	a = 88 b = 231 (R^2 = 0.50)	a = 109 b = 172 (R^2 = 0.50)
	Continuous CAP method	a = 87 b = 223 (R^2 = 0.55)	a = 115 b = 161 (R^2 = 0.59)
AUROC PDFF > 5%	*Prevalence*	32%	59%
	Standard CAP method	0.889 [0.827-0.953] Cutoff (Youden) = 273 dB/m	0.835 [0.745-0.924] Cutoff (Youden) = 264 dB/m
	Continuous CAP method	0.900 [0.838-0.961] Cutoff (Youden) = 286 dB/m	0.873 [0.798 – 0.949] Cutoff (Youden) = 256 dB/m
	Delong test p-value (difference)	0.55	0.06
	Delong test p-value (non-inferiority with a 0.02 margin)	0.02	<0.01

PDFF = proton density fat fraction; AUROC = area under the receiver operating characteristic,

R^2 = coefficient of determination

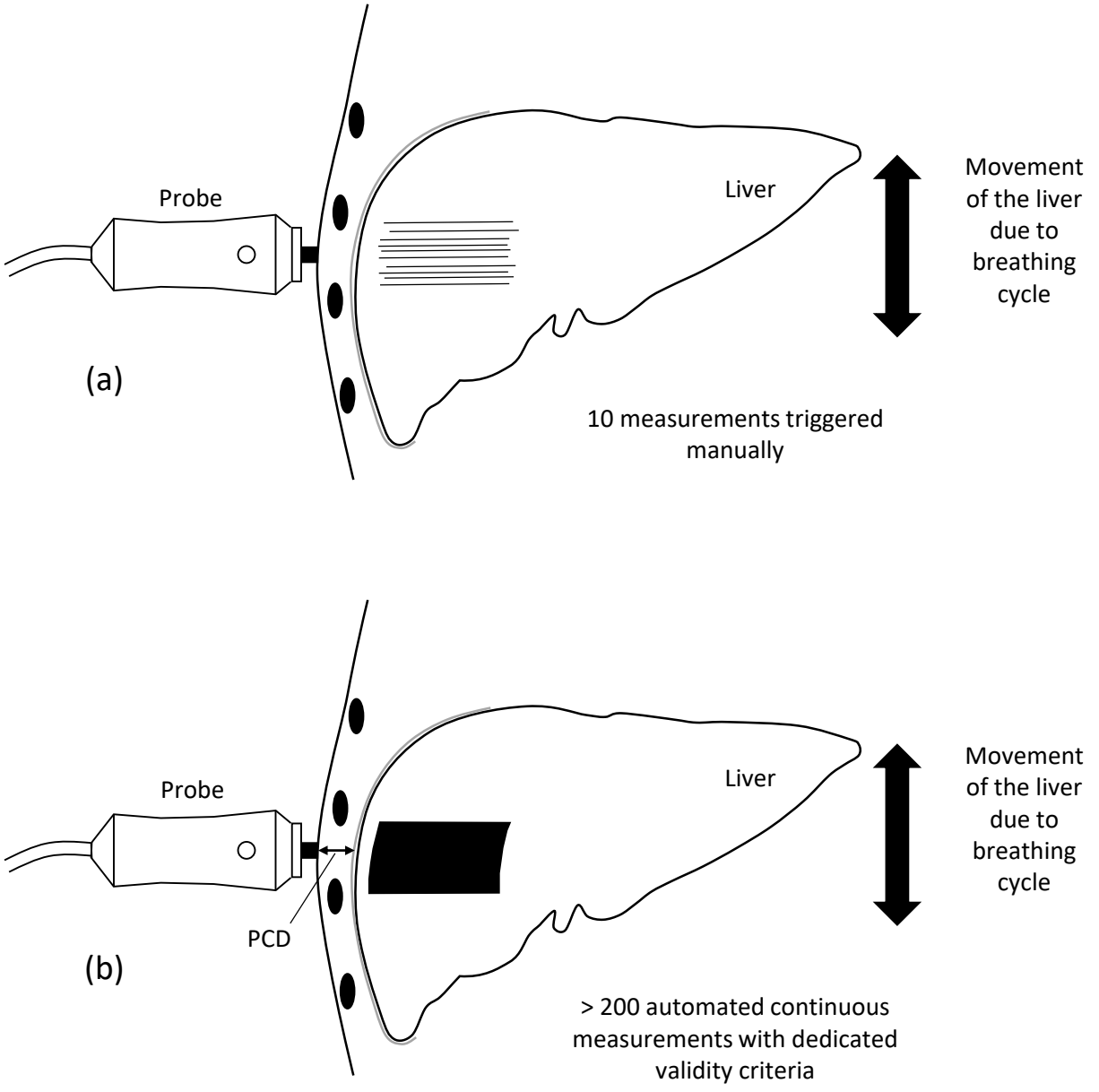

	Standard CAP method	Continuous CAP method
S Probe	**No data**	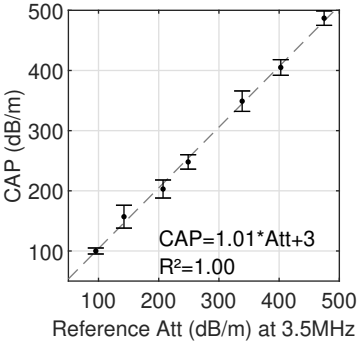
M Probe	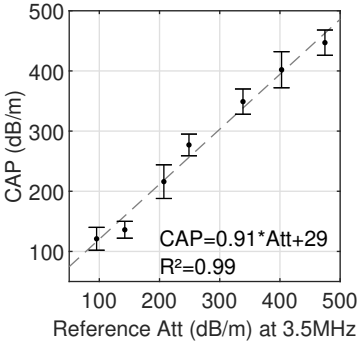	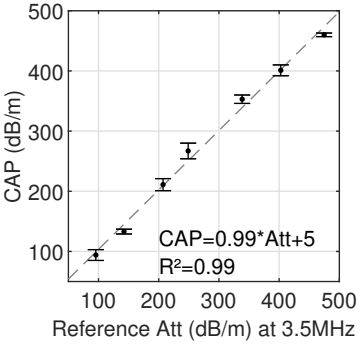
XL Probe	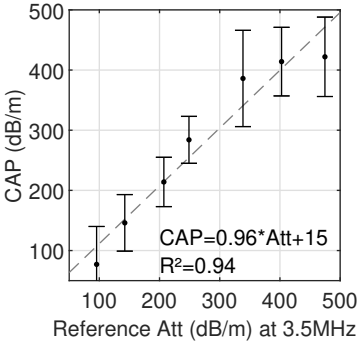	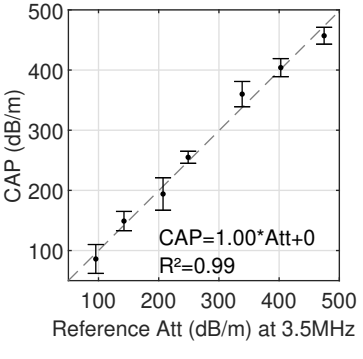

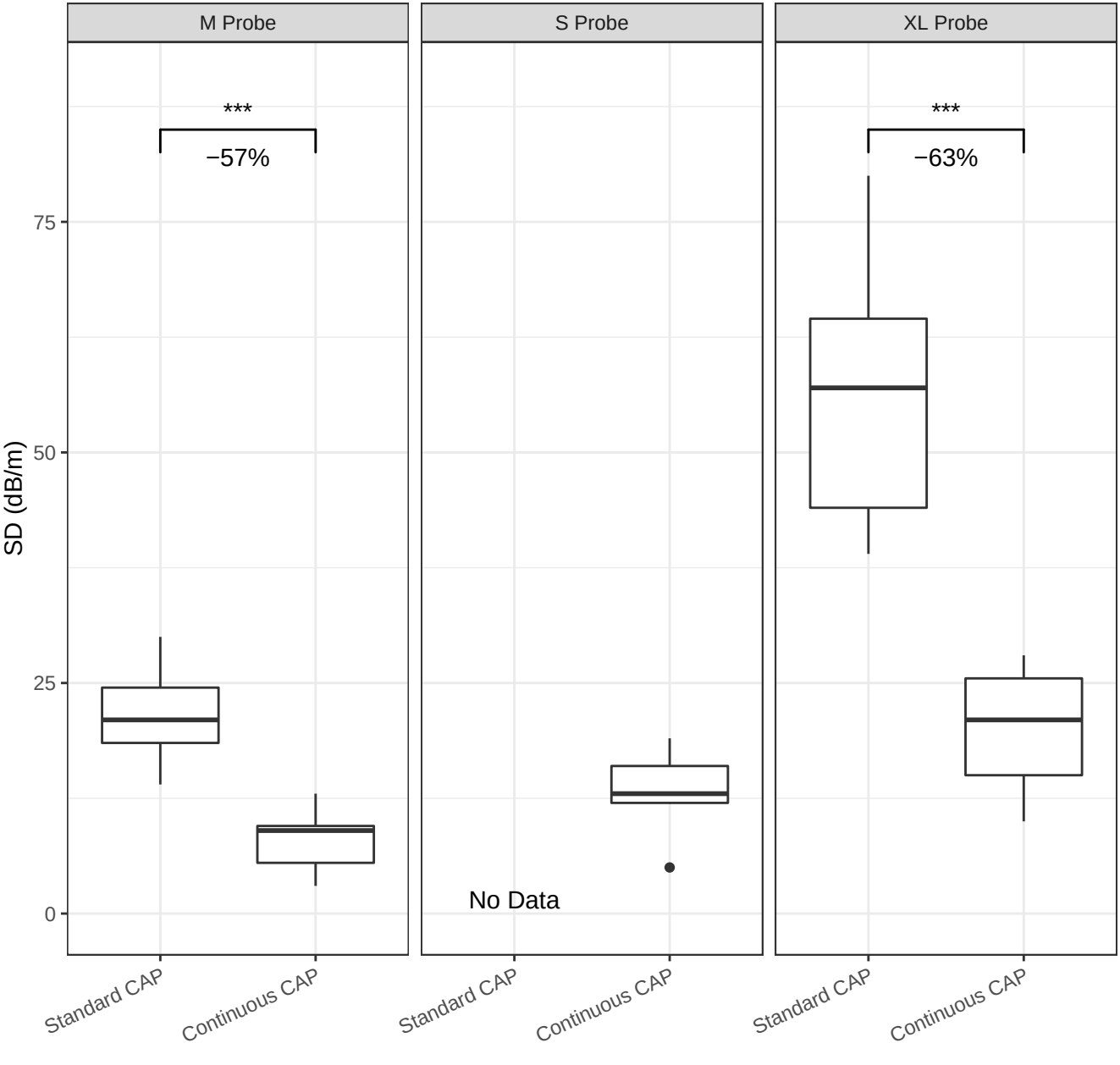

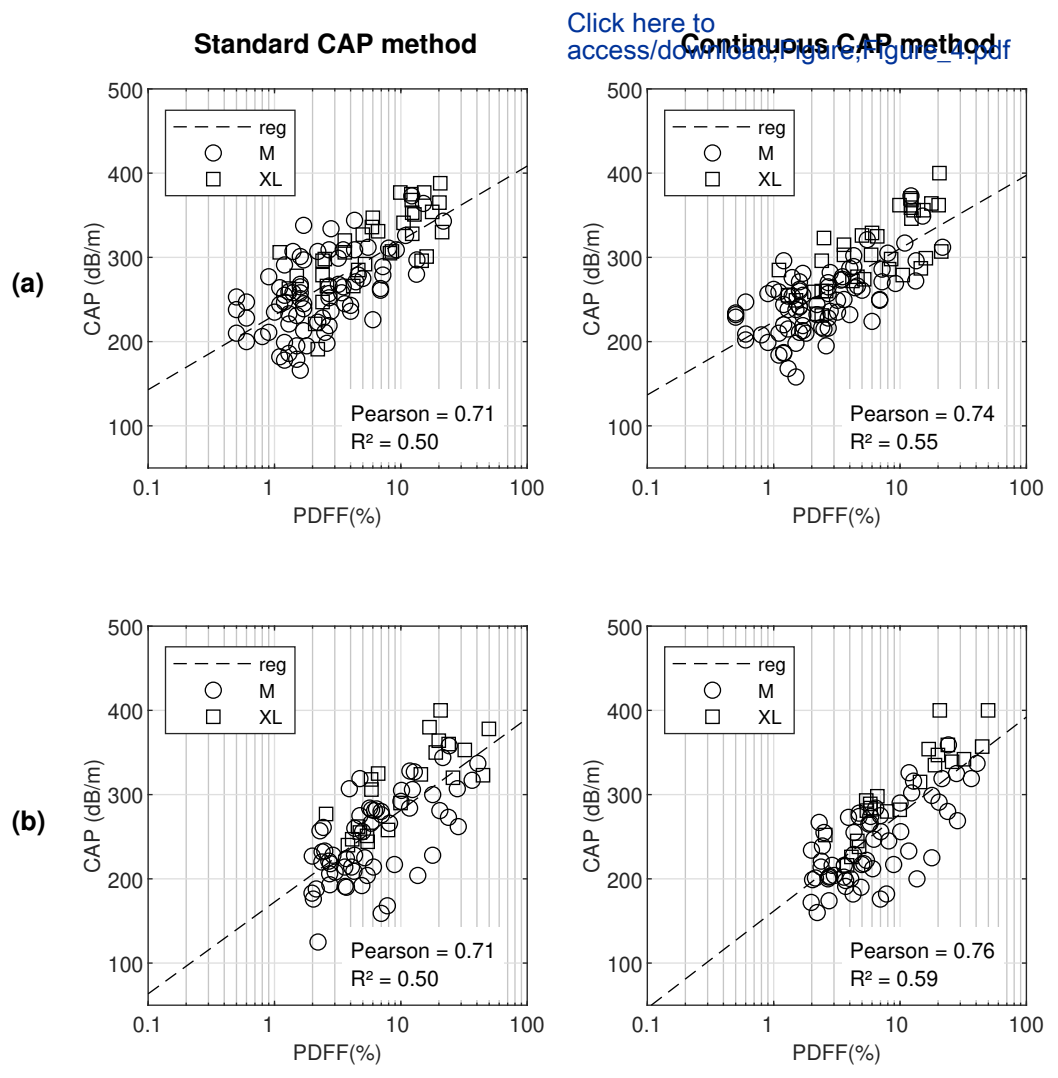

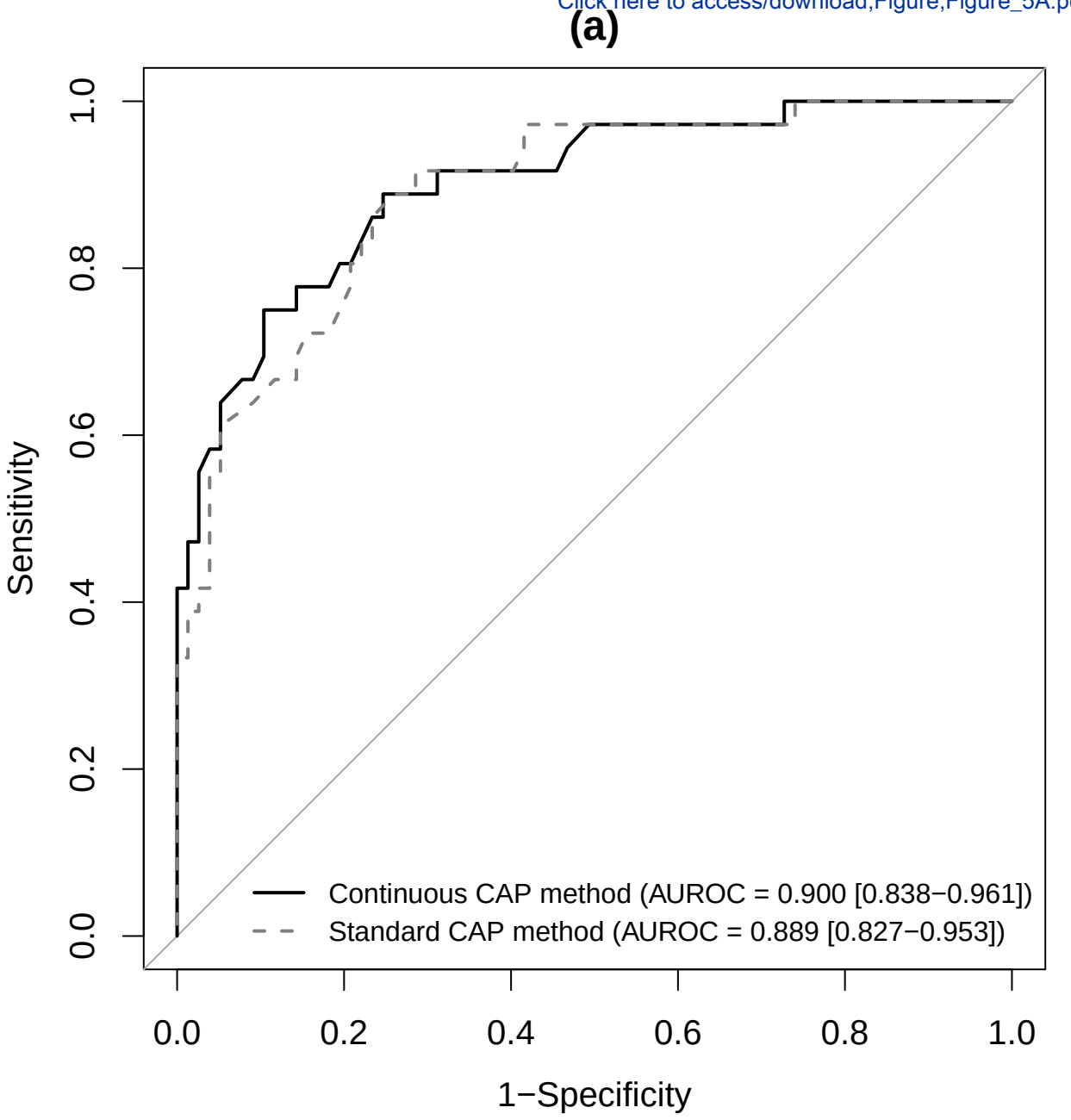

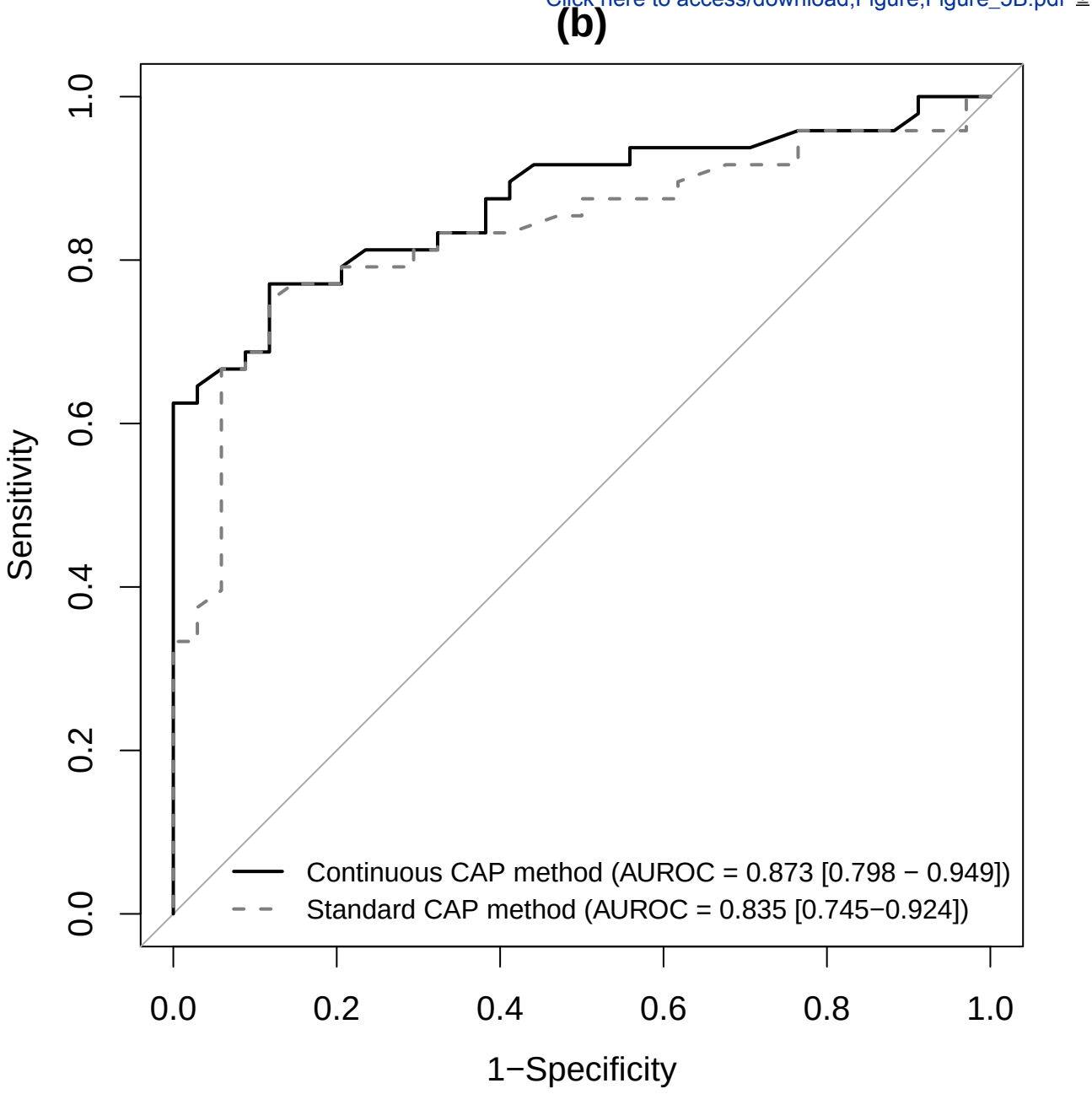

(a)

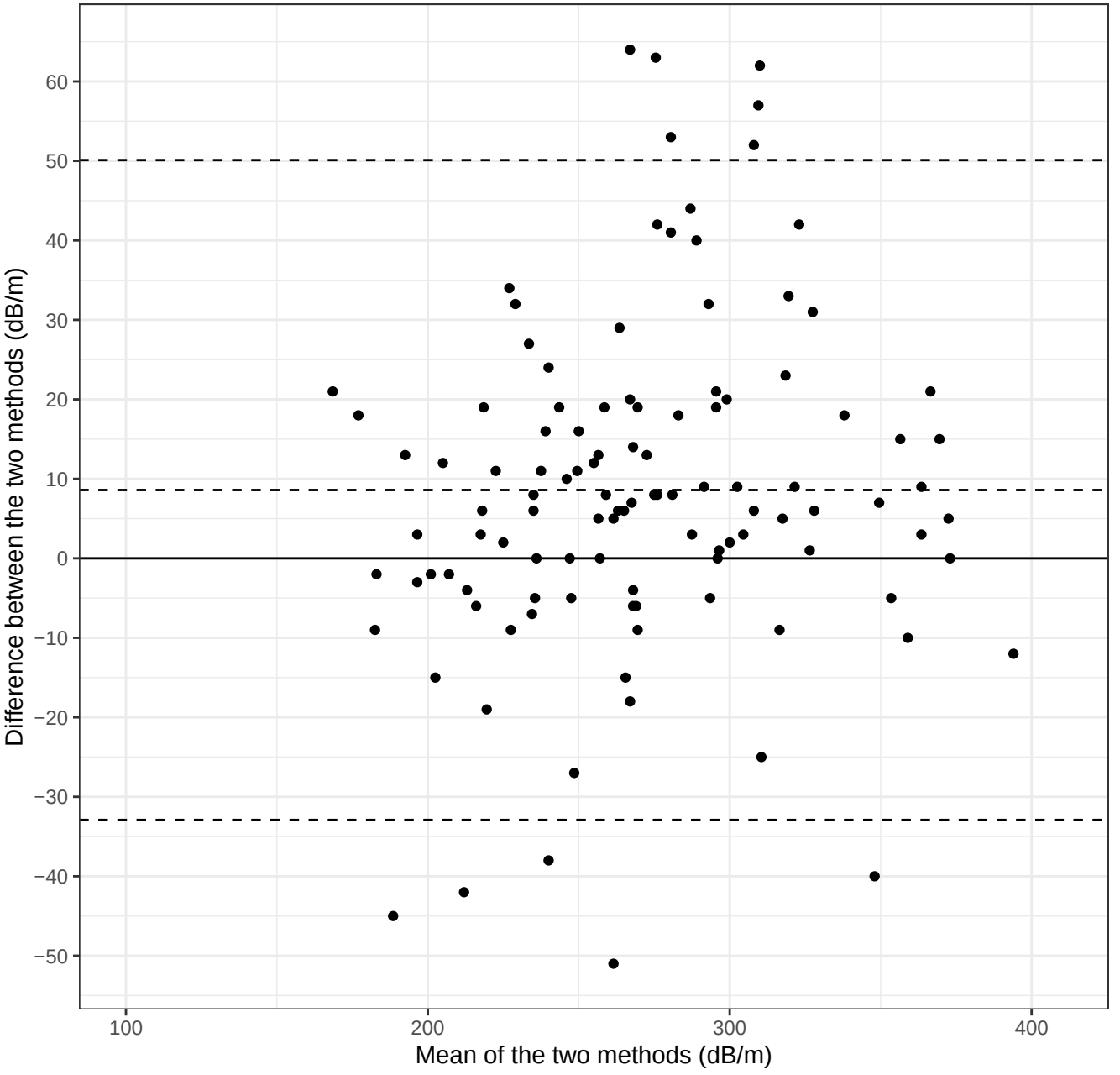

Figure

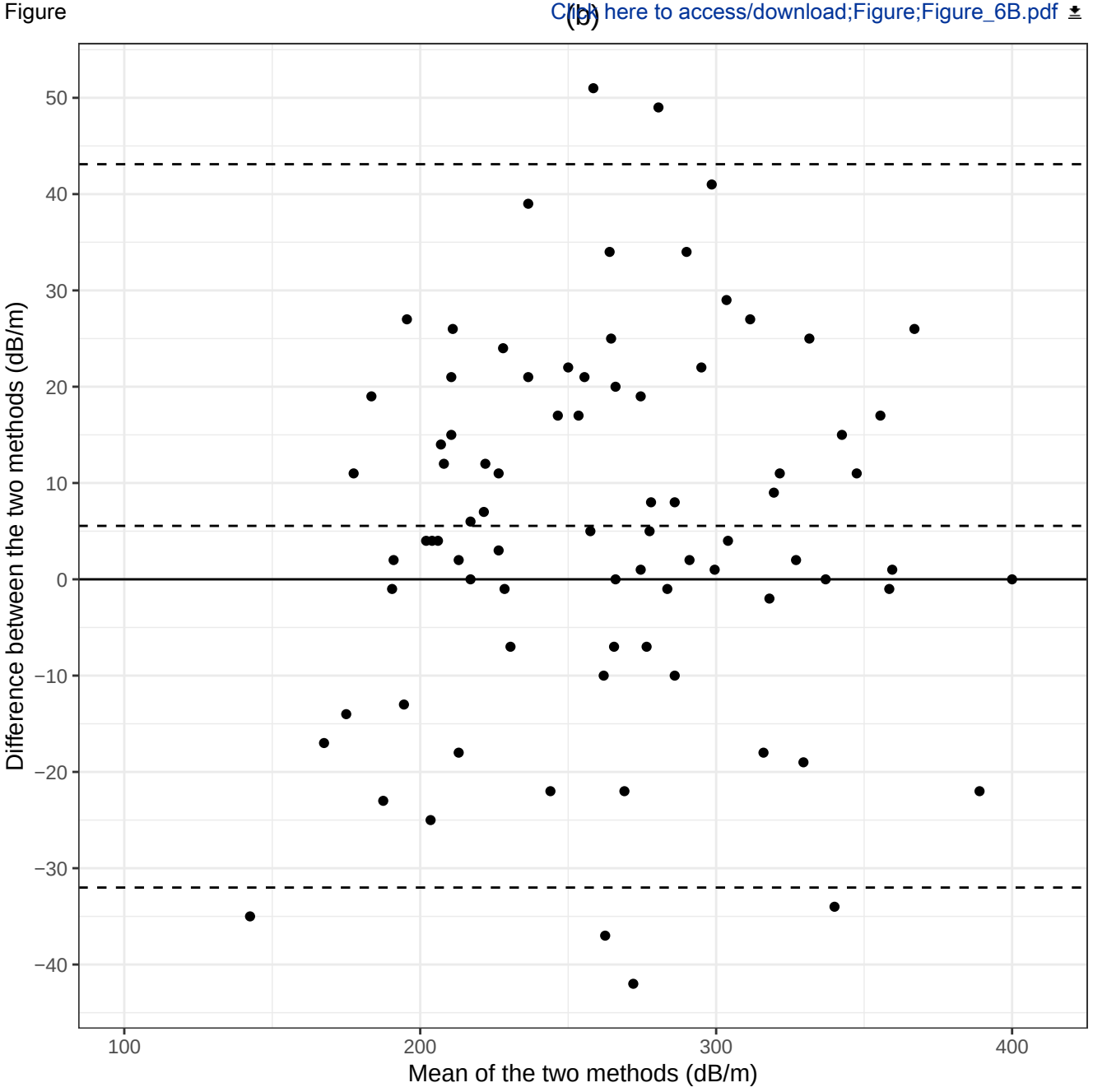

Figure

(a)

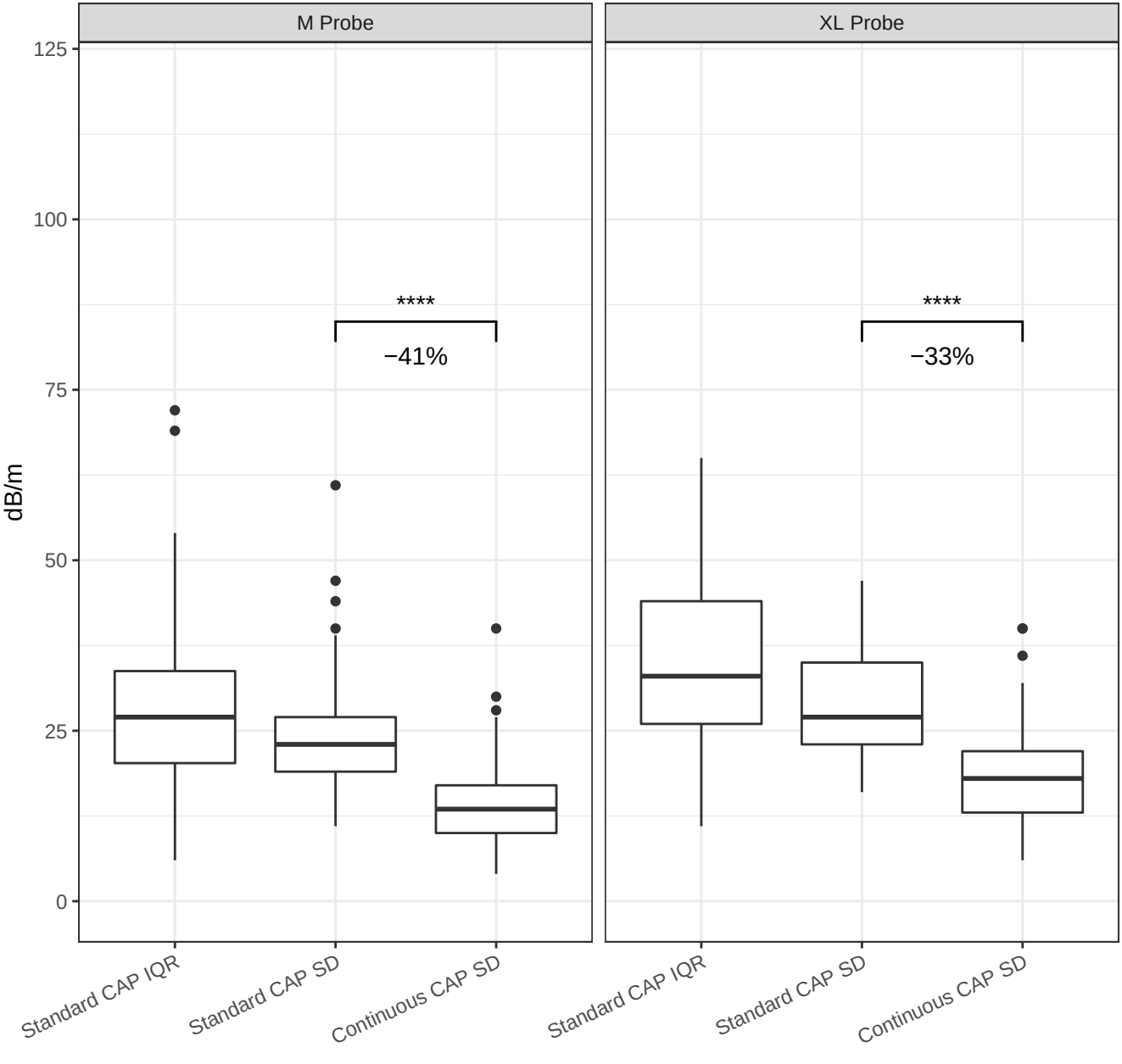

Figure

Click here to access/download;Figure;Figure_7B.pdf